

---

# An Overview of the First Principles DFT Exploration of Various Properties of the Individual Layers of Perovskite Solar Cells

K. Deepthi Jayan<sup>1,2\*</sup> and Varkey Sebastian<sup>1</sup>

DOI: 10.9734/bpi/aaer/v12/8864D

---

## ABSTRACT

The rapid improvement in efficiency of perovskite solar cells has made them the key to future developments in photovoltaics and their properties are of great interest to the academic community. Perovskites exhibit a host of intriguing properties, such as ferroelectricity, superconductivity, magnetoresistance, birefringence and piezoelectricity, due to their unique crystal structure. In comparison, perovskite solar cell performance has improved from 3.1 percent in 2009 to 24.4 percent in 2019. As a vast number of elements can be assembled to form perovskite structures, the physical, optical and electrical properties of perovskite can be engineered and optimized selectively. It is possible to access the previously unknown structural properties, opto-electronic properties and operating parameters of these materials with high precision through theoretical and analytical modeling. This paper seeks to describe a few abilities of DFT hybrid functionals to investigate the electronic, structural and optical properties of compounds that constitute different layers of a perovskite solar cell using software packages such as VASP, WIEN2k etc. The effect of doping on the electronic properties of different layers of perovskite solar cells, including band gap, visible light absorption, relaxation time of holes and electrons using DFT, is also examined in this paper which in turn defines the optimum separation of charge. The consequence of adding an intermediate band gap in the perovskite structure using  $G_0W_0$ +SOC approach-based DFT methods is also discussed here. A study on the impact of different intrinsic defects present in perovskite structures using VASP or WIEN2k package with DFT calculations is also discussed. The importance of modeling the interfaces of different layers of perovskite solar cells with DFT packages is explored with the aid of selected material examples and representative interfaces.

*Keywords: Density functional theory; dye sensitized solar cells; perovskite solar cells; computational modelling.*

## 1. INTRODUCTION

As a possible alternative to conventional non-renewable energy sources such as fossil fuels, renewable energy sources such as solar, biomass, geothermal, hydroelectric, wind, etc., which are generally ample in accessibility, have arisen to fulfill global energy needs. Because of its low cost, high performance, configurability, robustness and zero adverse environmental effects, solar energy has many advantages over other types of renewable energy. The relentless desire to enhance the performance of solar cells has contributed to the emergence of various heterostructures of semiconductors, thin films and other nanostructured materials that can function as possible candidates for the industrial production of solar cells. Even then, in order to develop modern high-efficiency solar cells, comprehensive knowledge of the electronic, mechanical, optical properties and chemical structure of various materials comprising distinct layers of solar cells is required. Owing to the combination of well-established numerical codes capable of representing the ground state

---

<sup>1</sup>Nirmalagiri College, Kannur University, Kannur, Kerala, 670701, India.

<sup>2</sup>Rajagiri School of Engineering & Technology (Autonomous), Rajagiri Valley, Kakkanad, Kochi, Kerala, 682039, India.

\*Corresponding author: E-mail: deepthijayan12@gmail.com;

properties of different materials, Density Functional Theory (DFT) has become highly popular in this regard [1]. Conventional approaches of electronic structure estimation aim to find optimal solution to the Schrödinger equation of  $N$  interacting electrons traveling in an external electrostatic potential, which has certain limitations arising from the requirement of tremendous computational efforts and the non-trivial nature of the problem itself. In DFT, an entirely different approach is employed, where the one-body electron density is chosen as the fundamental variable instead of the many-body wave equation [2].

While the Local Density Approximation (LDA) based on uniform distribution of electron density and the Generalized Gradient Approximation (GGA) based on non-uniform distribution of electron density are two best methods for estimating the electronic properties of compounds in the ground state, they do not provide reliable results for measurements of excited states of compounds [3,4]. On the other hand, with some improved mathematics and computational codes of DFT, hybrid approaches like B3LYP, PBE0, HSE and meta hybrid GGA attempt to integrate features from first-principle methods such as Hartree Fock techniques. The B3LYP hybrid method appears to be more reliable when working with computational chemistry applications than other hybrid DFT measurement methods, even though most of the hybrid methods rely on the materials of relevance. The HSE06, another DFT measurement technique is good for measuring band offsets, band gaps, etc., but it was noticed to have some drawbacks, especially when dealing with direct-indirect overlap as with the case of the alloy, GaAsP [5]. One of the Many Body Perturbation Theory (MBPT) approaches namely GW, can yield accurate results, especially when studying electronic and optical properties, and has the advantage of using it self- consistently [6-8]. Interfaces play a significant role in determining the overall chemical and physical properties of a heterojunction device. For the current low-cost PV technologies such as organic photovoltaics (OPV), dye sensitized solar cells (DSCs) and organometal halide perovskite solar cells, where nano-and mesostructured 3D interfaces are present, precise control at the interface level is of utmost importance. A Super Lattice Approximation is found to be the most accurate solution when interfaces are present as it can provide an indication of the band lineup [9]. Time Dependent DFT calculations can be used to calculate the frequency dependent molecular response properties like charge carrier transport and charge diffusion [10]. It can be used to study the absorption and energy loss spectra, photo ionization, high harmonic generation, photo emission etc. of many electron systems in time-dependent fields. DFT can indeed give insight on the notions of the materials' electronegativity, hardness and chemical reactivity index, and is important for evaluating the resilience of different perovskite materials [11].

In general, the optical properties measured by DFT show weak consistency with experimental findings, especially when logarithmic scale absorption coefficient ( $\alpha$ ) spectra are analyzed. If by integrating the energy scale correction by a hybrid functional, the optical function calculated from generalized gradient approximation (GGA) using very high-density  $k$  mesh is blue-shifted, then the estimated absorption spectra would be consistent with the experimental findings [12]. In particular, while determining photon absorption parameters, the dielectric properties of materials play a key role and can be estimated using the density functional perturbation theory [13-15]. An analysis of bonding and associated properties using DFT can be used to evaluate optical properties such as the complex second-order optical susceptibility dispersion tensor and their intra-and inter-band contributions and the multipole moments of compounds [16]. The polarization direction and the theoretical spectra of circular dichroism of materials can be studied with the help of Time Dependent Density Functional Theory [17]. Third-order components related to physical properties such as nonlinear electrical susceptibility, nonlinear elasticity or photo elastic and electro-strictive effects may be generated by a DFT approach combined with finite difference techniques and symmetry analysis [18]. DFT technique combined with different exchange correlation functionals allow the evaluation of absorption, reflectivity, optical conductivity and energy loss spectrum, in addition to exciton binding energies and corresponding optoelectronic properties such as ionization potentials and electron affinities [19].

## **2. COMPUTATIONAL MODELLING OF DYE SENSITIZED SOLAR CELLS (DSSCs)**

While inorganic solar cells based on silicon are commonly used because of their high performance, they are rigid and the cost of production is high. Soon after the groundbreaking work published by O'Regan and Gratzel in 1991, substantial research was undertaken to increase the performance of

solar cells, culminating in the manufacture of solar energy from renewable materials such as Dye Sensitized Solar Cells (DSSCs) [20-22]. Due to their low production costs, ease of processing, and light weight components, DSSCs are an essential form of thin film photovoltaic technology. Researchers have made efforts in recent years to create new and powerful sensitizers based on ruthenium complexes, zinc porphyrin, natural dyes and organic metal-free dyes, of which DSSCs relying on the first two substances have reached efficiencies well above 11% [23-26]. By improving the porosity of the electrode made of fine oxide powder, the performance can be improved so that dye absorption over the electrode could be enhanced and light harvesting efficiency could also be improved as a result [27]. With the help of Density Functional Theory (DFT) and Time Dependent Density Functional Theory (TD-DFT) methods, a thorough analysis and an accurate description of different properties of individual components and interfaces that comprise the critical components of Dye Sensitized Solar Cells (DSSCs) can be conducted and used to improve the performance parameters of the device [28]. Labat et al. successfully demonstrated that it is not only possible to measure the microscopic properties such as the electronic structure and optical properties, but also the global parameters such as the open circuit voltage ( $V_{oc}$ ) and the short circuit current density ( $J_{sc}$ ), quite accurately using a global hybrid functional (GH) approach such as B3LYP and PBE0 and a periodic approach for evaluation of dye-semiconductor and semiconductor-electrolyte interfaces [29-30].

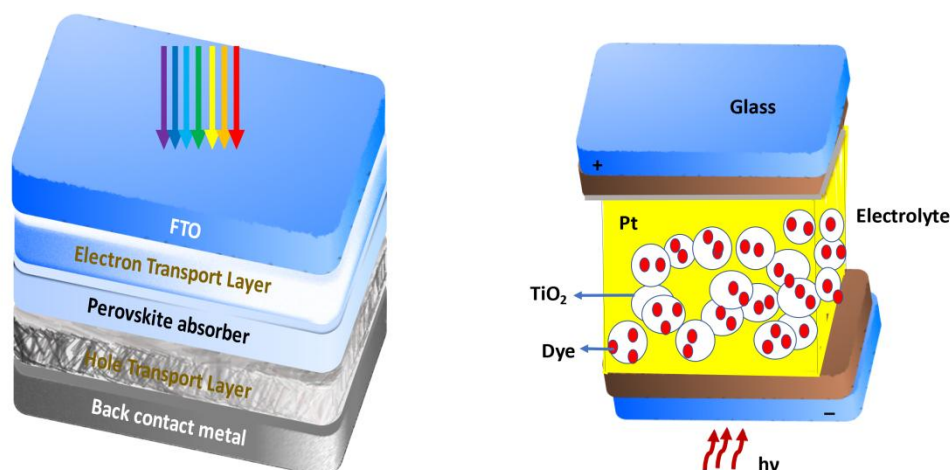


Fig. 1. Schematic diagram of perovskite solar cells (left) and DSSC (right)

## 2.1 Modelling of Individual Components and interfaces of DSSCs

For the optimum performance of DSSCs, a semiconductor material with a conduction band edge well below the excited state of the dye is typically required. It is evident from the references that a DFT study using Global Hybrid Functionals (GH) and periodic boundary conditions can provide a very accurate description of semiconductor electronic and structural properties as part of the DSSC assembly [31-32]. However, a good RSH functional performs better than a GH functional for the measurement of band gap, but HSE is not suitable for the analysis of excited state, since an accurate description of the excited state of both dye and semiconductor is necessary for excited state estimates [33]. Some studies show that the electronic properties of the dye compounds and their absorption spectrum can be well described using the exchange-correlation functional PBE0, which comes under the GH functional approach, while considering the solvent effects [34-35].

Interfacial engineering is important in heterojunction devices to achieve optimum device performance parameters. The dye molecule must be tightly bound to the semiconductor with the aid of different anchoring groups such as carboxylic moiety in order to achieve high performance and hence modeling the structural properties of different DSSC interfaces becomes very important [36]. The bi-isonicotinic acid (BINA) molecule as an anchoring group over an anatase (101) surface for the N<sub>3</sub>/TiO<sub>2</sub> system and a formic acid as an anchoring group over a wurtzite (1010) for the EY/ZnO DSSC system

demonstrate that both anchoring groups react in a dissociative fashion [37]. Similarly, the structural properties of two anchoring groups, acetylacetone and catechol, were recently studied for ZnO-based applications and it was found that these groups anchor the dye effectively to the surface [38, 39]. For modeling the actual dye/semiconductor interface using periodic boundary condition or any other modeling software package, the adsorption geometry obtained from the analysis of the sample systems can next be used. In order to perform a complete modelling of the DSSCs, an analysis of the electronic and structural properties of electrolyte-semiconductor interface is essential. Labat et al. studied the impact of electrolyte composition on DSSC open-circuit voltage ( $V_{oc}$ ) and found that if the Conduction Band Edge (CBE) energy is higher, a higher  $V_{oc}$  can be acquired [40].

### 3. COMPUTATIONAL MODELLING OF PEROVSKITE SOLAR CELLS (PSCs)

Apart from DSSCs, since the discovery of ceramic high-temperature superconductors to organic-inorganic semiconductors for high-efficiency photovoltaics, perovskite structures with the same crystal structure as  $\text{CaTiO}_3$  are of interest in the field of Materials Science and Engineering. In comparison, perovskite solar cell performance has improved from 3.1 % in 2009 to 25.2 % in 2019 [41]. The quest to produce highly effective and durable perovskite solar cells and to increase their overall efficiency is growing. A record Power Conversion Efficiency (PCE) above 22%, which is comparable to single crystalline Si solar cells, has been achieved by methyl ammonium lead iodide based solar cells. The stability of these solar cells when exposed to air, however, remains an obstacle to their commercialization. Using solid solutions or the mixing of two or more related elements at the A-site or X-site of perovskite structures is one way to increase stability [42]. Also, the performance can be improved by incorporating some inorganic elements to the organic part of the materials and also by incorporating suitable amount of mixed halide ions. The toxicity concerns of the lead-based perovskite structures can be eliminated/reduced by replacing/adding suitable compositions of non-toxic elements Ge, Sn etc. The morphology, structural properties, chemical properties, physical properties, thermal properties and stability can be improved by suitably modelling the different layers of the perovskite solar cells [43-45].

One of the methods to reduce the computational efforts for modelling solid solutions is to use a Super Cell (SC) method. With the pseudopotential plane wave technique, the Virtual Crystal Approximation (VCA) procedure can be used to reduce the computational cost, where the pseudopotential of the virtual atom is constructed by estimating the associated potential and wave functions of the constituent atoms [43]. The VCA method has been shown to be able to provide precise values of lattice constants in the cubic phase as a linear mixing content function, i.e. Vegard's law, although certain practical difficulties in measuring structural and electronic properties are present for hybrid halide perovskites [44,45]. After executing the structural optimization of supercells, a non-SCF measurement can be performed to obtain the electronic band configuration and density of states (DOS). Post-processing of the energy band will produce the effective masses of conductive electrons and holes. Bethe-Salpeter method can be used to estimate the frequency-dependent dielectric constants by considering the influence of electron-hole interaction and subsequently, the Density Functional Perturbation Theory (DFTB) can be used to figure out the optical properties such as exciton binding energy and absorption coefficient [46-48].

Through the Kohn-Sham equations, density functional theory reduces the quantum mechanical ground state many-electron problem to a self-consistent one-electron form [49]. This method is explicitly accurate, but the exchange-correlation energy as a density functional needs to be approximated for practical calculations. The normal LDA and GGA approximations typically underestimate the band gap of inorganic perovskite structures, since DFT is effectively a principle relevant for studying the ground state properties of materials. But for organic perovskites like methyl ammonium lead iodide, the PBE and PBEsol exchange correlation functional under the GGA approximation provides an accurate bandgap consistent with the experimental results [50]. The error due to the underestimated bandgap by GGA is cancelled for inorganic perovskite structures by the error arising from the overestimation of bandgap due to the lack of spin-orbit coupling and hence relativistic effects must be considered while evaluating the bandgap of a material [51, 52]. Using first-order Scalar Relativistic (SR) and higher order spin orbit coupling (SOC) contributions, relativistic effects can be accounted for. However, more complex approaches such as HSE06, which usually

overestimates the band gap of hybrid and all-inorganic perovskite structures, need to be adopted for estimating the bandgap. HSE06 can therefore provide a reasonable estimate of the band gap of inorganic perovskites by combining with SOC treatment [53]. It is possible to provide a precise description of the electronic structure in the excited state by integrating the GW approximation with many body interactions studies [54].

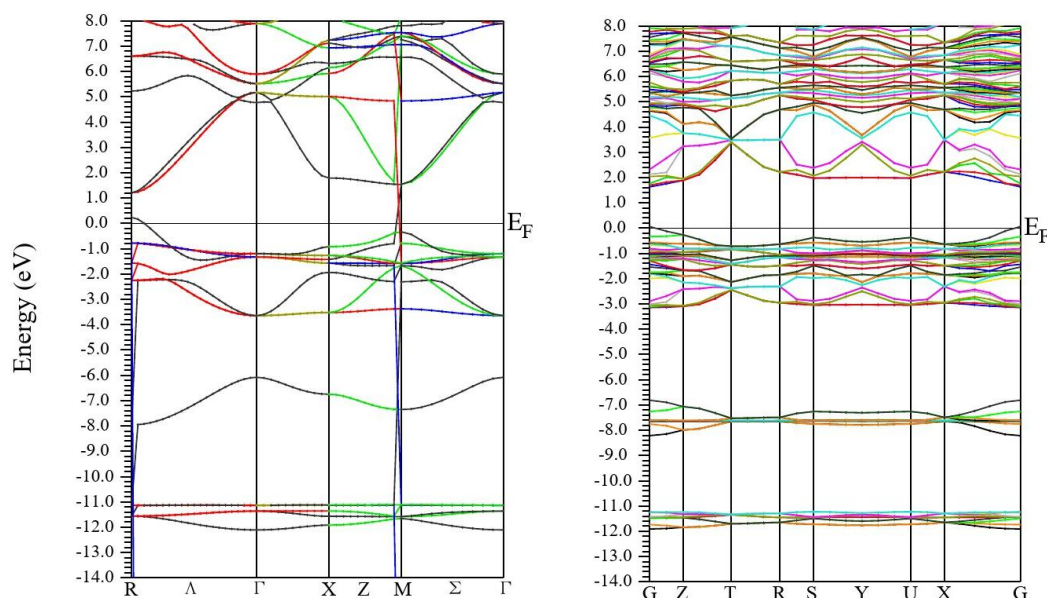


**Fig. 2. Electronic band structure of RbGeI<sub>3</sub> (left) and CsPbI<sub>3</sub> (right) with TB-mBJ exchange-correlation potential**

For methyl ammonium lead iodide, a small decrease in volume with the action of a small disturbance or a slight increase in pressure has been found to result not only in a decrease in the band gap in DFT calculations, but also a transition from an indirect to a direct band gap [55]. The effect of varying the temperature for the compound has not yet been well studied, although some studies indicate that a decline in temperature results in a decrease in the band gap of the perovskite structure [55]. The bandgap of the perovskite compounds largely depends on the A site and B site cations of the material, while the X site anions also directly influence the valence band positions. By changing the crystal structure due to the presence of its molecular orbitals much away from the Valence Band Limit (VBM), the A site cation seems to have an indirect effect only on the band gap, while substitution on the B-site cation will specifically alter the conduction band without any change in the entire crystal structure. As the X-site anion dominates the valence bands, the replacement on the X-site anion may be predicted to change the VBM [56]. Since the conduction electrons and holes combine to form excitons, charge carrier transport analysis is important in understanding the efficiency of the perovskite solar cells and can be performed with the incorporation of a van der Waals (vdW) correction with GW + SOC measurement [57]. Lejaeghere et al. provides numerous sources and descriptions of the various programming codes in which 40 different DFT approaches have been compared in order to achieve high-precision equation of state data [58].

### 3.1 Modelling of Hybrid and Inorganic Halide Perovskite

Using regular DFT with the assistance of (PBE) functional structural properties, the electronic composition, optical properties and stability of organo-metal halide perovskite structures can be studied effectively [59]. However, some studies show that the estimation of the MAPbI<sub>3</sub> band gap using SR DFT provides values in strong alignment with the experimental results, while MASnI<sub>3</sub> indicates a deviation of approximately 1 eV from the experimental results [60]. However, when the Spin Orbit Pairing is taken into account with DFT, there is an underestimation of the band gap for MAPbI<sub>3</sub>, which can be overcome by a GW technique integrating SOC [61]. This method results in a

great correlation with the SOC-GW absorption spectrum and experimental data when electron-hole interactions are ignored [62]. Compared to the absorption spectrum of  $\text{MAPbI}_3$ , a red shift in wavelength exists in the absorption range of  $\text{MASnI}_3$ , which specifically indicates that it is particularly acceptable for photovoltaic devices [59]. Dopants added to the absorber layer can improve the performance parameters of a perovskite solar cell, by inserting intermediate bandgaps into the existing band structure.

The intermediate band gaps can be introduced into the existing band structure by introducing suitable doping materials. Gregorio Garcia et al. have shown that the performance of perovskite solar cells can be improved by partially replacing Pb with Cr in methyl ammonium lead iodide (MAPI) perovskite, leading to the creation of an Intermediate Band Gap (IGB) with the desired properties, resulting in the absorption of two additional photons [63]. The band gap calculations with PBEsol+SOC, however, underestimates the value obtained experimentally [64]. In order to measure the MAPI bandgap doped with Cr ions, the  $G_0W_0$ +SOC method, which integrates spin orbit coupling effects, is then applied. The study of the band structure reveals that the displacement of one Cr atom instead of Pb results in two new energy levels due to the creation of Cr-3d orbital, which can serve as an IGB [65].

Defects, surfaces, and interfaces play an important role in deciding solar cell efficiency. In order to research the effect of such intrinsic defects as the Schottky defect or the Frenkel defect on solar cell efficiency, it is important to estimate the electronic structures and formation energies determined using the VASP (Vienna ab initio simulation) or WIEN2k software package with DFT [66]. For MAPI, plane waves with a cut-off energy of 520 eV are used to extend electronic wave functions and the projector-augmented wave (PAW) approach is used to explain the core-valence relationship [67]. In this study, the hybrid functional approach with PBE GGA as the exchange-correlation functional was used. For obtaining the bulk MAPI structure, the Monkhorst-Pack sampling with a  $4 \times 4 \times 4$  k point grid was chosen and with a  $2 \times 2 \times 2$  k-point grid for supercell calculation, the electronic structure was calculated. Another analysis using the VASP kit was performed by Youveri Wang et al. to estimate the structural and electronic properties using the plane-wave projector-augmented wave system with a  $4 \times 4 \times 4$  Monkhorst-pack k-mesh [68]. The van der Waals density function (vdW-DF) in the form of optB86b-vdW was used for structural relaxation, which explicitly offers details on the dispersion relationship between the organic base and the Pb-I system [69]. The electronic properties are studied by using the PBE functional and the modified Becke-Johnson (mBJ) potential by considering the SOC effect. Jishi et al. published a DFT based first-principles measurement of six separate lead halide semiconductors, namely,  $\text{CH}_3\text{NH}_3\text{PbI}_3$ ,  $\text{CH}_3\text{NH}_3\text{PbBr}_3$ ,  $\text{CsPbX}_3$  (X=Cl, Br, I), and  $\text{RbPbI}_3$  using the full potential linear augmented plane wave (LAPW) approach with WIEN2k package [70] and excellent agreement was achieved between the theoretical and experimental values of bandgap with modified Becke-Johnson (mBJ) exchange-correlation potential. The recent work of Liu et al. demonstrates the electronic and mechanical properties of MAPI doped with Cs that could act as a potential candidate for high efficiency perovskite photovoltaic materials [71].

Many DFT based studies have been done so far for analyzing the electronic, structural, optical, thermoelectric, thermodynamic and mechanical properties of pure and doped inorganic perovskite materials using DFT. Our study performed for  $\text{CsPbI}_3$ ,  $\text{CsSnI}_3$  and  $\text{RbGeI}_3$  inorganic perovskites using DFT indicate that these materials are suitable for photovoltaic activities. The bandstructure of these materials are shown in Fig. 2. Once the optical, mechanical, elastic and electronic properties of the perovskite absorber materials are estimated with DFT, a complete modelling of the perovskite solar cell (PSC) and the subsequent performance optimization can be done using SCAPS 1D software package by incorporating various organic or inorganic materials for the transport layers. We have done a complete modelling of PSC with methyl ammonium tin iodide ( $\text{MASnI}_3$ ) as the absorber layer for diverse transport materials and back contact metals. A high PCE of 25.05% was achieved for the solar cell device configuration Glass/FTO/PCBM/ $\text{MASnI}_3$ /CuI/Au, with the organic PCBM as the electron transport layer, the inorganic CuI as the hole transport layer and Au as the back contact metal with a work function of 5.1 eV [72].

### 3.2 Modelling of Hole Transporters

The Hole Transport Layer (HTL) plays a significant role in perovskite solar cells for the conversion of photovoltaic energy. The most popular HTL for perovskite-based solar cells is the organic Spiro-

MeOTAD [2,2',7,7'-tetrakis-(N,N-di-4-methoxyphenylamino)-9,9'-spirobifluorene], but for DSSC, Co(II)/Co(III) redox shuttles act as the most suitable HTL [70]. One of the key reasons for using spiro-MeOTAD as HTL is that the radical cation has two oxidation states, 2+ and 4+, with long-term stability in both states. A study of the excited spiro-MeOTAD-derived cation states in the absorption processes carried out with the help of DFT and TDDFT reveals that optimum photon absorption occurs in the visible region of the oxidized species [73]. While estimating the electronic, optical and structural properties, a good agreement between the theoretical and experimental results is observed for both the neutral and oxidized forms and hence spiro MeOTAD is suitable as HTL in both PSCs and DSSCs. The functional exchange-correlation of B3LYP can be used to refine the vacuum structure of SpiroMeOTAD and its oxidized forms (spiro-MeOTAD<sup>+</sup>, spiro-MeOTAD<sup>2+</sup> and spiro-MeOTAD<sup>4+</sup>) without taking any symmetry requirements into consideration. The spin-adapted configurations were considered by Simona Fantacci et al. and DFT calculations such as UB3LYP calculations were conducted for the SpiroMeOTAD mono- and di cations [74].

### 3.3 Modelling of Electron Transporters

Modelling of the parameters of the electron transport layers using DFT is also needed for improving the photovoltaic output parameters of the solar cell. Car-Parrinello molecular dynamics play an important role at finite temperatures in the sampling of local minima and dynamic fluctuations. The DFT/TDDFT structure can be used as the most critical method to research the desired materials and interfacial properties, as discussed earlier. The first theoretical modeling of perovskite solar cells based on TiO<sub>2</sub> and Al<sub>2</sub>O<sub>3</sub> was conducted by Ali Akbari et al. and it was observed that the perovskite interfacial plane greatly affects the energy level alignment between TiO<sub>2</sub> and perovskite, resulting in the bending of the mesoporous perovskite solar cell bands relative to planar perovskite solar cells [75]. It was inferred from this analysis that Al<sub>2</sub>O<sub>3</sub> is not appropriate for producing perovskite solar cells and the addition of Al<sub>2</sub>O<sub>3</sub> makes the perovskite solar cells extremely unstable [76].

### 3.4 Modelling of Interfaces and Surfaces

Power conversion efficiency, stability and hysteresis of Perovskite solar cells are often influenced by the presence of interfaces. Mosconi and co-workers investigated TiO<sub>2</sub> to MAPI and MAPbI<sub>3-x</sub>Cl<sub>x</sub> interfaces with a limited Cl material of about 4 percent with the aid of SOC-DFT calculations [77]. DFT electronic structure calculations revealed that, due to the interaction of perovskite with TiO<sub>2</sub>, there is a strong interfacial coupling between the 3D conduction band states of Ti and 6p conduction band states of Pb. It was concluded that the same relationship resulted in a small improvement in TiO<sub>2</sub> conduction band energy. The presence of defects at the interfaces has also been observed to change the band alignment, contributing to the bending of perovskite bands near to the TiO<sub>2</sub> surface, resulting in the production of trap states. Qian et al. also studied the CsPbBr<sub>3</sub>/TiO<sub>2</sub> heterostructure using the PBEsol+HSE06 functional to explain the cases of all-inorganic perovskites and observed that a broad charge transfer takes place between Cs and O atoms, while a smaller charge transfer between Br and Ti atoms takes place owing to the presence of interface defects [78].

## 4. CONCLUSION

A theoretical review focused on first principles DFT computation of structural properties, electronic and optical properties, material stability, effect of defects, surfaces and interfaces on hybrid organic-inorganic and purely inorganic halide perovskites is presented. While studies are successfully carried out on band gap tuning, band gap engineering, defect analysis etc., topics such as photon percolation into the interface and its effect on the overall performance of PSCs remain unattended. For Pb-free perovskite structures, the doping technique has barely been explored and further investigation for a specific composition is expected to bring about significant improvements in photovoltaic science.

## ACKNOWLEDGEMENT

The author acknowledges the faculty members of the Department of Physics, Nirmalagiri College, Kannur University, for their endless support, guidance and encouragement.



## COMPETING INTERESTS

Authors have declared that no competing interests exist.

## REFERENCES

1. Even J, et al. Density functional theory simulations of semiconductors for photovoltaic applications: hybrid organic-inorganic perovskites and III/V heterostructures. *International Journal of Photoenergy*. 2014;1-11.  
Available:<https://doi.org/10.1155/2014/649408>
2. Kurth S, Marques MAL, Gross EKV. Density functional theory. *Encyclopedia of Condensed Matter Physics*2005;395-40.  
Available:<https://doi.org/10.1016/B0-12-369401-9/00445-9>
3. Perdew JP, Wang Y. Accurate and simple analytic representation of the electron-gas correlation energy. *Physical review B: Condensed Matter and Materials Physics*. 1992;98: 13244–13249.  
Available:<https://doi.org/10.1103/PhysRevB.45.13244>
4. Perdew JP, Burke K, Ernzerhof M. Generalized Gradient Approximation Made Simple *Physical Review Letters*.1996;77:3865–3868.  
Available:<https://doi.org/10.1103/PhysRevLett.77.3865>
5. Nicklas JW, Wilkins JW. Accurate ab initio predictions of III–V direct-indirect band gap crossovers. *Applied Physics Letters*. 2010;97:091902–091902.  
Available:<https://doi.org/10.1063/1.3485297>
6. Surh MP, Louie SG, Cohen ML. Quasiparticle energies for cubic BN, BP, and BAs. *Physical Review B: Condensed Matter and Materials Physics*. 1991;43:9126–9132.  
Available:<https://doi.org/10.1103/PhysRevB.43.9126>
7. Chimot N, Even J, Folliot H, Loualiche S. Structural and electronic properties of BAs and BxGa<sub>1-x</sub>As, BxIn<sub>1-x</sub>As alloys. *Physica B: Condensed Matter*. 2005;364:263–272.  
Available:<https://doi.org/10.1016/j.physb.2005.04.022>
8. Prodhomme P, Fontaine-Vive F, Geest AVD, Blaise P. Even J. *Applied Physics Letters*. 2011;99:022101.  
Available:<https://doi.org/10.1063/1.3609869>
9. Prodhomme P, Fontaine-Vive F, Geest AVD, Blaise P, Even J. Ab initio calculation of effective work functions for a TiN/HfO<sub>2</sub>/SiO<sub>2</sub>/Si transistor stack. *Applied Physics Letters*. 2011;99:022101.  
Available:<https://doi.org/10.1063/1.3609869>
10. van Gisbergen SJA, Osinga VP, Grijsenko OV, van Leeuwen R, Snijders JG, Baerends EJ. Improved density functional theory results for frequency-dependent polarizabilities, by the use of an exchange-correlation potential with correct asymptotic behavior. *Journal of Chemical Physics*. 1996;105:3142–3151.  
Available:<https://doi.org/10.1063/1.472182>
11. Kohn W, Becke AD, Parr RG. Ternary tetradymite compounds as topological insulators. *J. Phys. Chem*. 1996;100:12974–12980.  
Available:<https://doi.org/10.1021/jp960669l>
12. Nishiwaki M, Fujiwara H. Highly accurate prediction of material optical properties based on density functional theory. *Computational Materials Science*. 2020;172:109315.  
Available:<https://doi.org/10.1016/j.commatsci.2019.109315>
13. Baroni S, Gianozzi P, Testa A. Elastic constants of crystals from linear-response theory. *Physical Review Letters*. 1987;59:2662.  
Available:<https://doi.org/10.1103/PhysRevLett.59.2662>
14. Gonze X, Vigneron JP. Density-functional approach to nonlinear-response coefficients of solids. *Physical Review B: Condensed Matter and Materials Physics*. 1989;39: 13120–13128.  
Available:<https://doi.org/10.1103/PhysRevB.39.13120>
15. Gonze X, Amadon B, Anglade PM, et al. ABINIT: First-principles approach to material and nanosystem properties. *Computer Physics Communications*. 2009;180:2582–2615.  
Available:<https://doi.org/10.1016/j.cpc.2009.07.007>
16. Merad Boudia I, Reshak AH, Ouahrani T, Bentalha Z. Density functional theory calculation of the optical properties and topological analysis of the electron density of MBi<sub>2</sub>B<sub>2</sub>O<sub>7</sub> (M= Ca, Zn) compounds. *Journal of Applied Physics*. 2013;113: 083505.



- Available:<https://doi.org/10.1063/1.4792733>
17. Mori T, Inoue Y, Grimme S. Experimental and Theoretical Study of the CD Spectra and Conformational Properties of Axially Chiral 2, 2 '-, 3, 3 '-, and 4, 4 '-Biphenol Ethers. *The Journal of Organic Chemistry*. 2006;71:9797–9806.  
Available:<https://doi.org/10.1021/jo061855i>
  18. Pedesseau L, Katan C, Even J. On the entanglement of electrostriction and non-linear piezoelectricity in non-centrosymmetric materials. *Applied Physics Letters*. 2012;100:031903.  
Available:<https://doi.org/10.1063/1.3676666>
  19. Lee JC, Chai JD, Lin ST. Assessment of density functional methods for exciton binding energies and related optoelectronic properties. *RSC Advances*. 2015;5:101370–101376.  
Available:<https://doi.org/10.1039/C5RA20085G>
  20. O'Regan B, Gratzel M. A low-cost, high-efficiency solar cell based on dye-sensitized colloidal TiO<sub>2</sub> films. *Nature*. 1991;353:737–740.  
Available:<https://doi.org/10.1038/353737a0>
  21. Hagfeldt A, Boschloo G, Sun L, Kloo L, Pettersson H. Dye sensitized solar cells. *Chem. Rev*. 2010;110:6595–6663.  
Available:<https://doi.org/10.1021/cr900356p>
  22. Spitler MT, Parkinson BA. Dye sensitization of single crystal semiconductor electrodes. *Acc. Chem. Res*. 2009;42:2017–2029.  
Available:<https://doi.org/10.1021/ar900232m>
  23. Wang XF, Tamiaki H. Cyclic tetrapyrrole based molecules for dye-sensitized solar cells. *Energy Environ. Sci*. 2010;3:94–106.  
Available:<https://doi.org/10.1039/B918464C>
  24. Campbell WM, Jolley KW, Wagner P, Wagner K, Walsh PJ, Gordon KC, Schmidt-Mende L, Nazeeruddin MK, Wang Q, Gratzel M, et al. tzet, DL Officer. *J. Phys. Chem. C*. 2007;111:11760–11762.  
Available:<https://doi.org/10.1021/jp0750598>
  25. Dong H, Zhou X, Jiang C. Molecular design and theoretical investigation on novel porphyrin derivatives for dye-sensitized solar cells. *Theor. Chem. Acc*. 2012;131:1102.  
Available:<https://doi.org/10.1007/s00214-012-1102-5>
  26. Planells M, Pelleja L, Clifford JN, Pastore M, De Angelis F, Lopez N, Marder SR, Palomares E. Energy levels, charge injection, charge recombination and dye regeneration dynamics for donor–acceptor  $\pi$ -conjugated organic dyes in mesoscopic TiO<sub>2</sub> sensitized solar cells. *Energy Environ. Sci*. 2011;4:1820–1829.  
Available:<https://doi.org/10.1039/c1ee01060c>
  27. Sharma K, Sharma V, Sharma SS. Dye-sensitized solar cells: fundamentals and current status. *Nanoscale Research Letters*. 2018;13:1-46.  
Available:<https://doi.org/10.1186/s11671-018-2760-6>
  28. Labat F, Le Bahers T, Ciofini I, Adamo C. First-principles modeling of dye-sensitized solar cells: Challenges and perspectives. *Accounts of Chemical Research*. 2012;45:1268–1277.  
Available:<https://doi.org/10.1021/ar200327w>
  29. Labat L, Baranek Ph, Adamo C. Structural and electronic properties of selected rutile and anatase TiO<sub>2</sub> surfaces: an ab initio investigation. *J. Chem. Theory Comput*. 2008;4:341–352.  
Available:<https://doi.org/10.1021/ct700221w>
  30. Labat F, Baranek P, Domain C, Minot C, Adamo C. Density functional theory analysis of the structural and electronic properties of TiO<sub>2</sub> rutile and anatase polytypes: Performances of different exchange-correlation functionals. *J. Chem. Phys*. 2007;126:154703.  
Available <https://doi.org/10.1063/1.2717168>
  31. Labat L, Baranek Ph, Adamo C. Structural and electronic properties of selected rutile and anatase TiO<sub>2</sub> surfaces: an ab initio investigation. *J. Chem. Theory Comput*. 2008;4:341–352.  
Available:<https://doi.org/10.1021/ct700221w>
  32. Cora F, Alfredsson M, Mallia G, Middlemiss DS, Mackrodt WC, Dovesi R, Orlando R. Principles and Applications of Density Functional Theory in Inorganic Chemistry II. *Struct. Bonding (Berlin)*. 2004;113:171–232.  
Available:<https://doi.org/10.1007/b97944>

33. Heyd J, Scuseria G. Efficient hybrid density functional calculations in solids: Assessment of the Heyd–Scuseria–Ernzerhof screened Coulomb hybrid functional. *J. Chem. Phys.* 2004;121:1187–1192.  
Available:<https://doi.org/10.1063/1.1760074>
34. Guillemoles JF, Barone V, Joubert L, Adamo CC. A theoretical investigation of the ground and excited states of selected Ru and Os polypyridyl molecular dyes. *J. Phys. Chem. A.* 2002;106:11354–11360.  
Available:<https://doi.org/10.1021/jp021517v>
35. Rekhis M, Labat F, Ouamerali O, Ciofini I, Adamo C. Theoretical analysis of the electronic properties of N<sub>3</sub> derivatives. *J. Phys. Chem.* 2008;A 111:13106–13111.  
Available:<https://doi.org/10.1021/jp075597k>
36. Labat F, Laine PP, Ciofini I, Adamo A. Spectral properties of bipyridyl ligands by time-dependent density functional theory. *Chem. Phys. Lett.* 2006;417:445–451.  
Available:<https://doi.org/10.1016/j.cplett.2005.10.066>
37. Labat F, Adamo C. Bi-isonicotinic acid on anatase (101): insights from theory. *J. Phys. Chem. C.* 2007;111:15034–15042.  
Available:<https://doi.org/10.1021/jp074349l>
38. Le Bahers T, Pauport\_e T, Labat F, Lef\_evre G, Ciofini I. Acetylacetone, an interesting anchoring group for ZnO-based organic–inorganic hybrid materials: a combined experimental and theoretical study. *Langmuir.* 2011;27:3442–3450.  
Available:<https://doi.org/10.1021/la103634v>
39. Le Bahers T, Pauport\_e T, Labat F, Odobel F, Ciofini I. Promising anchoring groups for ZnO-based hybrid materials: A periodic density functional theory investigation. *Int. J. Quantum Chem.* 2012;112:2062–2071.  
Available:<https://doi.org/10.1002/qua.23134>
40. Le Bahers T, Labat F, Pauport\_e T, Ciofini I. Effect of solvent and additives on the open-circuit voltage of ZnO-based dye-sensitized solar cells: a combined theoretical and experimental study. *Phys. Chem. Chem. Phys.* 2010;12:14710–14719.  
Available:<https://doi.org/10.1039/c004358c>
41. NREL Efficiency charts.  
Available:<https://www.nrel.gov/pv/assets/pdfs/cell-pv-eff-emergingpv.202001042.pdf>
42. Ono LK, Juarez-Perez EJ, Qi Y. Progress on perovskite materials and solar cells with mixed cations and halide anions. *ACS Appl. Mater. Interfaces.* 2017;9:30197–246.  
Available:<https://doi.org/10.1021/acsami.7b06001>
43. Íniguez J, Bellaiche LD. First-principles study of (BiScO<sub>3</sub>)<sub>1-x</sub>–(PbTiO<sub>3</sub>)<sub>x</sub> piezoelectric alloys. *Phys. Rev. B.* 2003;67:224107.  
Available:<https://doi.org/10.1103/PhysRevB.67.224107>
44. Jong UG, Yu CJ, Ri JS, Kim NH, Ri GC. Influence of halide composition on the structural, electronic, and optical properties of mixed CH<sub>3</sub>NH<sub>3</sub>Pb(I<sub>1-x</sub>Br<sub>x</sub>)<sub>3</sub> perovskites calculated using the virtual crystal approximation method. *Phys. Rev. B.* 2016;94:125139.  
Available:<https://doi.org/10.1103/PhysRevB.94.125139>
45. Jon UG, Yu CJ, Jang YM, Ri GC, Hong SN, Pae YH. Revealing the stability and efficiency enhancement in mixed halide perovskites MAPb(I<sub>1-x</sub>Cl<sub>x</sub>)<sub>3</sub> with ab initio calculations. *J. Power Sources.* 2017;350:65–72.  
Available:<https://doi.org/10.1016/j.jpowsour.2017.03.038>
46. Baroni S, de Gironcoli S, Dal Corso A, Giannozzi P. Phonons and related crystal properties from density-functional perturbation theory. *Rev. Mod. Phys.* 2001;73:515–62.  
Available:<https://doi.org/10.1103/RevModPhys.73.515>
47. Sharma S, Dewhurst JK, Ambrosch-Draxl CC. Validity of effective-medium theory for optical properties of embedded nanocrystallites from ab initio supercell calculations. *Phys. Rev. B.* 2003;67:165332.  
Available:<https://doi.org/10.1103/PhysRevB.67.165332>
48. Onida G, Reining L, Rubio A. Electronic excitations: density-functional versus many-body Green's-function approaches. *Rev. Mod. Phys.* 2002;74:601–59.  
Available:<https://doi.org/10.1103/RevModPhys.74.601>
49. Kohn W, Becke AD, Parr RG. Density functional theory of electronic structure. *J. Chem. Phys.* 1996;100:12974.

- Available:<https://doi.org/10.1021/jp960669l>
50. Perdew JP, Burke K, Ernzerhof M. D. of physics and NOL 70118. Phys. Rev. Lett. 1996;77:3865.  
Available:<https://doi.org/10.1103/PhysRevLett.77.3865>
  51. Even J, Pedesseau L, Katan C. Analysis of multivalley and multibandgap absorption and enhancement of free carriers related to exciton screening in hybrid perovskites. J. Phys. Chem. C. 2014;118:11566–72.  
Available:<https://doi.org/10.1021/jp503337a>
  52. Azarhoosh P, McKechnie S, Frost JM, Walsh A, van Schilfgaarde M. Research Update: Relativistic origin of slow electron-hole recombination in hybrid halide perovskite solar cells. APL Mater. 2016;4:091501.  
Available:<https://doi.org/10.1063/1.4955028>
  53. Heyd J, Scuseria GE, Ernzerhof M. Hybrid functionals based on screened coulomb potential. J. Chem. Phys. 2003;118:8207–15 ().  
Available:<https://doi.org/10.1063/1.1564060>
  54. Brivio F, Butler KT, Walsh A, van Schilfgaarde M. Relativistic quasiparticle self-consistent electronic structure of hybrid halide perovskite photovoltaic absorbers. Phys. Rev. B. 2014;89:155204 ().  
Available:<https://doi.org/10.1103/PhysRevB.89.155204>
  55. Wang T, Daiber B, Frost JM, Mann SA, Garnett EC, Walsh A, Ehrler B. Indirect to direct bandgap transition in methylammonium lead halide perovskite. Energy & Environmental Science. 2017;10:509-515.  
DOI:10.1039/C6EE03474H
  56. Yamada Y, Nakamura. Near-band-edge optical responses of solution-processed organic–inorganic hybrid perovskite  $\text{CH}_3\text{NH}_3\text{PbI}_3$  on mesoporous  $\text{TiO}_2$  electrodes. Appl. Phys. Express. 2014;7:032302.  
Available:<https://doi.org/10.7567/APEX.7.032302>
  57. Lindblad R, Jena NK, Philippe B, Oscarsson J, et al. Electronic structure of  $\text{CH}_3\text{NH}_3\text{PbX}_3$  perovskites: dependence on the halide moiety. J. Phys. Chem. C. 2015;119:1818–25.  
Available:<https://doi.org/10.1021/jp509460h>
  58. Umari P, Mosconi E, De Angelis F. Relativistic GW calculations on  $\text{CH}_3\text{NH}_3\text{PbI}_3$  and  $\text{CH}_3\text{NH}_3\text{SnI}_3$  perovskites for solar cell applications. Sci. Rep. 2014;4:4467.  
Available:<https://doi.org/10.1038/srep04467>
  59. Lejaeghere K, Bihlmayer G, Björkman T, Blaha P, Blügel S, Blum V, Caliste D, Castelli IE, Clark SJ, Dal Corso A, De Gironcoli S. Reproducibility in density functional theory of solids. Science. 2016;351:aad3000.  
Available:<https://doi.org/10.1126/science.aad3000>
  60. Burschka J, Pellet N, Moon SM, Humphry-Baker R, Gao P, Nazeeruddin MK, Grätzel M. Sequential deposition as a route to high-performance perovskite-sensitized solar cells. Nature. 2013;499:316–319.  
Available:<https://doi.org/10.1038/nature12340>
  61. Castelli IE, Olsen T, Datta S, Landis DD, Dahl S, Thygesen KS, Jacobsen KW. Computational Screening of Perovskite Metal Oxides for Optimal Solar light capture. Energy Environ. Sci. 2012;5:814–5819.  
Available:<https://doi.org/10.1039/C1EE02717D>
  62. Even J, Pedesseau L, Jancu JM, Katan C. Importance of Spin–Orbit Coupling in Hybrid Organic/Inorganic Perovskites for Photovoltaic Applications. J. Phys. Chem. Lett. 2013;4:2999–3005.  
Available:<https://doi.org/10.1021/jz401532q>
  63. Umari P, Mosconi E, De Angelis F. Relativistic GW calculations on  $\text{CH}_3\text{NH}_3\text{PbI}_3$  and  $\text{CH}_3\text{NH}_3\text{SnI}_3$  perovskites for solar cell applications. Sci. Rep. 2014;4:4467.  
Available:<https://doi.org/10.1038/srep04467>
  64. Yu CJ. Advances in modelling and simulation of halide perovskites for solar cell applications. Journal of Physics: Energy. 2019;1:022001.  
Available:<https://doi.org/10.1088/2515-7655/aaf143>

65. García G, Palacios P, Menéndez-Proupin E, Montero-Alejo AL, Conesa JC, Wahnón P. Influence of chromium hyperdoping on the electronic structure of  $\text{CH}_3\text{NH}_3\text{PbI}_3$  perovskite: a first-principles insight. *Scientific Reports*. 2018;8:1-12.  
Available:<https://doi.org/10.1038/s41598-018-20851-x>
66. Kresse G, Hafner J. Ab initio molecular dynamics for liquid metals. *Phys. Rev. B*. 1993;47:558.  
Available:<https://doi.org/10.1103/PhysRevB.47.558>
67. Blöchl PE. Projector augmented wave method. *Phys. Rev. B*. 1994;50:17953–17979.  
Available:<https://doi.org/10.1103/PhysRevB.50.17953>
68. Wang Y, Zhang Y, Zhang P, Zhang W. High intrinsic carrier mobility and photon absorption in the perovskite  $\text{CH}_3\text{NH}_3\text{PbI}_3$ . *Physical Chemistry Chemical Physics*. 2015;17:11516–11520.  
Available:<https://doi.org/10.1039/C5CP00448A>
69. Klimes J, Bowler DR, Michaelides A. Van derWaals density functionals applied to solids. *Phys. Rev. B*. 2011;83:195131.  
Available:<https://doi.org/10.1103/PhysRevB.83.195131>
70. Jishi RA, Ta OB, Sharif AA. Modeling of lead halide perovskites for photovoltaic applications. *The Journal of Physical Chemistry C*. 2014;118:28344–28349.  
Available:<https://doi.org/10.1021/jp5050145>
71. Liu D, Li S, Bian F, Meng X. First-principles investigation on the electronic and mechanical properties of Cs-doped  $\text{CH}_3\text{NH}_3\text{PbI}_3$ . *Materials*. 2018;11:1141.  
Available:<https://doi.org/10.3390/ma11071141>
72. Jayan KD, Sebastian V. Comprehensive device modelling and performance analysis of  $\text{MASnI}_3$  based perovskite solar cells with diverse ETM, HTM and back metal contacts. *Solar Energy*. 2021;217:40-48.  
Available:<https://doi.org/10.1016/j.solener.2021.01.058>
73. Hawash Z, Ono LK, Qi Y. Recent Advances in Spiro-MeOTAD Hole Transport Material and Its Applications in Organic–Inorganic Halide Perovskite Solar Cells. *Advanced Materials Interfaces*. 2018;5.  
Available:<https://doi.org/10.1002/admi.201700623>
74. Fantacci S, De Angelis F, Nazeeruddin MK, Grätzel MM. Electronic and Optical Properties of the Spiro-MeOTAD Hole Conductor in Its Neutral and Oxidized Forms: A DFT/TDDFT Investigation. *The Journal of Physical Chemistry C*. 2011;115:23126–23133.  
Available:<https://doi.org/10.1021/jp207968b>
75. Akbari A, Hashemi J, Mosconi E, De Angelis F, Hakala M. First principles modelling of perovskite solar cells based on  $\text{TiO}_2$  and  $\text{Al}_2\text{O}_3$ : stability and interfacial electronic structure. *Journal of Materials Chemistry A*. 2017;5:2339-2345.  
Available:<https://doi.org/10.1039/C6TA08874K>
76. de Angelis F. Modeling materials and processes in hybrid/organic photovoltaics: from dye-sensitized to perovskite solar cells. *Accounts of Chemical Research*. 2014;47(3):349–3360.
77. Mosconi E, Ronca E, de Angelis F. First-principles investigation of the  $\text{TiO}_2$ /organohalide perovskites interface: The role of interfacial chlorine. *The Journal of Physical Chemistry Letters*. 2014;5:2619–2625.  
Available:<https://doi.org/10.1021/jz501127k>
78. Qian CX, Deng ZY, Yang K, Feng J, Wang MZ, Yang Z, Liu S, Feng HJ. Interface engineering of  $\text{CsPbBr}_3/\text{TiO}_2$  heterostructure with enhanced optoelectronic properties for all-inorganic perovskite solar cells. *Applied Physics Letters*. 2018;112:093901.  
Available:<https://doi.org/10.1063/1.5019608>

---

© Copyright (2021): Author(s). The licensee is the publisher (B P International).

**DISCLAIMER**

This chapter is an extended version of the article published by the same author(s) in the following Conference Proceedings. AIP Conference Proceedings, 2162, 020036, 2019.